Protein Component of *Bacillus subtilis* RNase P Specifically Enhances the Affinity for Precursor-tRNA^{Asp} †

Jeffrey C. Kurz, S. Niranjanakumari, and Carol A. Fierke*

Department of Biochemistry, Box 3711, Duke University Medical Center, Durham, North Carolina 27710

Received October 13, 1997

ABSTRACT: Ribonuclease P (RNase P) is an endonuclease that cleaves precursor tRNA to form the 5′-end of mature tRNA and is composed of a catalytic RNA subunit and a small protein subunit. The function of the protein component of *Bacillus subtilis* RNase P in catalysis of *B. subtilis* precursor tRNA^{Asp} cleavage has been elucidated using steady-state kinetics, transient kinetics, and ligand affinity measurements to compare the functional properties of RNase P holoenzyme to RNase P RNA in 10 mM $MgCl_2$, 100 mM NH_4Cl. The protein component modestly affects several steps including ≤10-fold increases in the rate constant for tRNA dissociation, the affinity of tRNA, and the rate constant for phosphodiester bond cleavage. However, the protein principally affects substrate binding, increasing the affinity of RNase P for pre-tRNA^{Asp} by a factor of 10^4 as determined from both the ratio of the pre-tRNA^{Asp} dissociation and association rate constants measured in 10 mM $MgCl_2$ and a binding isotherm measured in 10 mM $CaCl_2$ using gel filtration to separate enzyme-bound and free pre-tRNA^{Asp}. Therefore, the main role of the protein component in RNase P is to facilitate recognition of pre-tRNA by enhancing the interaction between the enzyme and the 5′-precursor segment of the substrate, rather than stabilizing the tertiary structure of the folded RNA as has been observed for protein-facilitated group I intron self-splicing. Furthermore, the protein component maximizes the efficiency of RNase P under physiological conditions and minimizes product inhibition.

Ribonuclease P (RNase P)[1] catalyzes the essential 5′-maturation of precursor tRNA by hydrolysis of a specific phosphodiester bond (*1*). Bacterial RNase P is a complex consisting of an RNA subunit (∼400 nucleotides; 130 kDa) and a small protein subunit (∼120 amino acids; 14 kDa). The RNA component efficiently catalyzes the cleavage reaction in vitro in the presence of nonphysiological high concentrations of salt (*2*), demonstrating that the RNA contains most of the determinants for binding and cleavage of substrates. However, the protein component facilitates cleavage by RNase P under physiological salt concentrations (*2, 3*) and appears to be required for efficient tRNA processing in vivo (*4*).

The involvement of essential protein factors in RNA-catalyzed reactions has also been observed for the in vivo self-splicing reactions of group I and group II introns (*5*−*7*). Furthermore, the *Neurospora* mitochondrial tyrosyl-tRNA synthetase (CYT-18 protein) and the yeast CBP2 protein induce folding of group I introns by binding specifically to RNA tertiary structures (*8*−*11*). A similar role has been proposed for the protein subunit of bacterial RNase P, which also appears to recognize the folded structure of the catalytic RNA (*2, 12*−*15*).

Previously, a kinetic and thermodynamic analysis was used to determine a complete kinetic scheme for the RNase P RNA-catalyzed cleavage of precursor tRNA^{Asp} (pre-tRNA^{Asp}) from *Bacillus subtilis* at high salt (*16*). These results provided an essential background for analysis of the effects of Mg^{2+}, another important cofactor, on substrate and product binding, and catalysis by RNase P RNA (*17*). We have used the same approach to obtain estimates of the rate constants describing the pathway of pre-tRNA^{Asp} cleavage catalyzed by *B. subtilis* RNase P holoenzyme at low salt. By comparison with the RNase P RNA-catalyzed reaction under identical conditions, we have shown that the protein component of RNase P specifically enhances the affinity of pre-tRNA^{Asp} compared to tRNA^{Asp}, thus increasing k_{cat}/K_M without increasing product inhibition under physiological conditions. Contrary to the role of proteins in group I intron self-splicing, the protein component of RNase P is essential for substrate recognition rather than RNA folding.

MATERIALS AND METHODS

RNA Preparation and Quantification. The RNA component of *B. subtilis* RNase P and *B. subtilis* pre-tRNA^{Asp} (containing 35 nucleotides 5′ to the RNase P processing site) were prepared by in vitro transcription from linearized plasmids using T7 RNA polymerase, as described (*16*).

† Supported by National Institutes of Health Grant GM 55387. J.C.K. was supported in part by NIH Training Grant GM 08487.

* To whom correspondence should be addressed. Telephone: (919)-684-2557. FAX: (919)-684-8885.

[1] Abbreviations: RNase P, ribonuclease P; Tris, tris(hydroxymethyl)-aminomethane; MES, 2-(*N*-morpholino)ethanesulfonic acid; EDTA, (ethylenedinitrilo)tetraacetic acid; TE buffer, 10 mM Tris-HCl, 1 mM EDTA, pH 8; SDS, sodium dodecyl sulfate; buffer 1, 10 mM $MgCl_2$, 100 mM NH_4Cl, 50 mM Tris-HCl, pH 7.8; buffer 2, 10 mM $MgCl_2$, 100 mM NH_4Cl, 50 mM Tris, 50 mM MES, pH 6.1; S or pre-tRNA^{Asp}, precursor tRNA^{Asp}; 5′P, 5′-precursor tRNA fragment; RNase P RNA, RNA component of RNase P; RNase P protein, protein component of RNase P; E, RNase P RNA or RNase P holoenzyme; cpm, counts per minute.

S0006-2960(97)02530-0 CCC: $15.00
Published on Web 02/06/1998

Products of the in vitro transcription reactions were separated by electrophoresis over a denaturing polyacrylamide gel (6−8% polyacrylamide, 7 M urea) (*18*), isolated by passive elution of gel fragments into a solution of TE (10 mM Tris-HCl, 1 mM EDTA, pH 8.0) containing 0.1% sodium dodecyl sulfate (SDS), and further purified by ethanol precipitation followed by gel filtration (*16*). RNAs were quantified by measuring the absorbance at 260 nm (*16*).

Radiolabeled pre-tRNA^{Asp} was produced posttranscriptionally by incorporation of a labeled phosphate group at the 5′ terminus of the transcript. The pre-tRNA^{Asp} was incubated with calf intestinal alkaline phosphatase (USB) to hydrolyze 5′-triphosphate groups resulting from the in vitro transcription reaction and 5′ end-labeled using T4 polynucleotide kinase (NEB) and [γ-^{32}P]ATP. Alternatively, uniformly labeled pre-tRNA^{Asp} was produced by inclusion of [α-^{32}P]GTP in the in vitro transcription reaction (*16*). ^{32}P-Labeled mature tRNA^{Asp} was prepared from uniformly labeled pre-tRNA^{Asp} by incubation of the precursor with RNase P RNA (*16*). Labeled RNAs were purified as described for unlabeled RNAs (*16*).

Protein Purification. The recombinant protein component of *B. subtilis* RNase P was expressed in BL21(DE3) pLysS pPWT1 by growth at 37 °C to an OD_{600} of 0.6−0.8, induction by the addition of 0.4 mM isopropyl β-D-thiogalactoside, and incubation at 37 °C for 4 h (Niranjanakumari and Fierke, unpublished data). The cells were lysed using a French press, and the protein was purified from the soluble fraction of the cell lysate by ammonium sulfate precipitation, followed by chromatography on G-50 Sephadex gel filtration and CM-Sepharose ion-exchange columns (Kurz and Fierke, unpublished data). The RNase P protein is >95% pure as assayed by SDS−polyacrylamide gel electrophoresis (*18, 19*). The purified protein (1 μM) does not cause degradation of labeled pre-tRNA^{Asp} in 5 mM $MgCl_2$, 100 mM NH_4Cl, 50 mM Tris-HCl, pH 8, over a period of 4 h, suggesting that the protein preparation is free from nonspecific ribonuclease contamination.

Steady-State Experiments. Steady-state turnover measurements of RNase P activity were performed under conditions of excess substrate ([S]/[E] ≥ 5) in buffer 1 (10 mM $MgCl_2$, 100 mM NH_4Cl, 50 mM Tris-HCl, pH 7.8, 37 °C) or buffer 2 [10 mM $MgCl_2$, 100 mM NH_4Cl, 50 mM Tris (Research Organics, ultrapure), 50 mM MES (SigmaUltra), pH 6.1, 37 °C]. Before the reaction, each type of RNA was heated for 3 min at 95 °C in TE, mixed with an equal volume of 2× buffer 1 or 2, and preincubated at 37 °C for 15 min. Holoenzyme was reconstituted by adding a slight molar excess of RNase P protein (in 10 mM Tris-HCl, pH 8) to RNase P RNA after the first 5 min of preincubation. Reactions were initiated by addition of RNase P to pre-tRNA^{Asp}, and the mixture was incubated at 37 °C. Time points (5 μL) were removed and quenched into an equal volume of stop mix [10 M urea, 200 mM EDTA (pH 8.0), 0.05% bromophenol blue, and 0.05% xylene cyanol]. Uncleaved pre-tRNA^{Asp} was separated from mature tRNA^{Asp} and 5′-precursor (5′P) on an 8% polyacrylamide gel containing 7 M urea, and these products were visualized and quantified using a Phosphorimager from Molecular Dynamics.

Single-Turnover Experiments. Experiments measuring single turnovers were performed and analyzed exactly as described for the steady-state experiments except that the enzyme was in excess ([E]/[S] ≥ 5) and the pH was decreased to 6.1 (buffer 2). For the E·pre-tRNA^{Asp} partitioning experiments, holoenzyme (400 nM) and ^{32}P-labeled pre-tRNA^{Asp} (*pre-tRNA^{Asp}; 1−2 nM) in buffer 2 were mixed and incubated as described for the steady-state turnover experiments. The reaction was incubated 2−10 s (t_1) at 37 °C, sufficient time to form E·*pre-tRNA^{Asp}. An aliquot was then removed and mixed with 9 volumes of a mixture containing excess unlabeled yeast tRNA type X (Sigma), to rapidly "trap" free holoenzyme as E·tRNA, and a slight excess of free RNase P protein (final concentrations: 40 nM RNase P RNA, 60−100 nM RNase P protein, and 100 μM unlabeled tRNA). This mixture was incubated for 14 s (t_2) at 37 °C, sufficient time for all the E·*pre-tRNA^{Asp} either to dissociate or to cleave (see Scheme 2), before the reaction was stopped by the addition of EDTA/urea. As a control, the amount of free *pre-tRNA^{Asp} cleaved during the tRNA trap step (t_2) was determined as approximately 10% from mixing an aliquot of RNase P (5 μL) with the tRNA prior to the addition of 5 μL *pre-tRNA^{Asp} and incubation at 37 °C. Product concentrations in the E·*pre-tRNA^{Asp} partitioning experiments were corrected for this incomplete trapping.

Binding Studies. The affinity of mature tRNA^{Asp} for RNase P RNA and holoenzyme was measured in the presence of 10 mM $MgCl_2$ and 10 mM $CaCl_2$ using a G-75 Sephadex centrifuge column assay, as described (*16*). RNase P RNA, holoenzyme, and uniformly labeled tRNA^{Asp} were prepared as described above in buffer 1 or 2 containing 10 mM $MgCl_2$ or $CaCl_2$ as indicated. Binding reactions containing 0.1 nM tRNA^{Asp} and excess RNase P (0.02−50 μM) were incubated at 37 °C for 10−60 min. After centrifugation, the amounts of radioactivity in the column matrix and eluate were separately quantified by scintillation counting. In principle, high molecular weight species (such as E·tRNA) will appear in the eluate after centrifugation while lower molecular weight species (such as tRNA) are retained in the gel matrix (*16, 20*). In practice, approximately 20% of the radioactivity elutes in the absence of enzyme ($cpm_{background}$) while approximately 80% elutes at high concentrations of RNase P ($cpm_{end\ point}$). The fraction of tRNA^{Asp} bound ([E·tRNA]/[$tRNA_{tot}$]) was calculated as ($cpm_{eluate} - cpm_{background}$)/($cpm_{end\ point} - cpm_{background}$).

Binding of end-labeled pre-tRNA^{Asp} to RNase P RNA or holoenzyme in buffer 2 (10 mM $CaCl_2$) was assayed as described for mature tRNA^{Asp}. Here approximately 35% of the radioactivity eluted in the absence of enzyme while the end point was 80% for holoenzyme and 65% for RNase P RNA.

Data Analysis. Kinetic and thermodynamic data were fit with the Kaleidagraph (Synergy Software) curve-fitting program using the equations listed below (*16, 21, 22*); the results are summarized in Scheme 1 or Table 1 with the standard errors. For multiple-turnover reactions, the initial velocity of product appearance was analyzed (≤10% of pre-tRNA^{Asp} cleaved). The steady-state kinetic parameters were determined by fitting initial velocities to the Michaelis−Menten equation (*23*).

The dissociation constants of RNase P for tRNA^{Asp} and pre-tRNA^{Asp} were determined by fitting the centrifuge column data to eq 1, where L represents either tRNA^{Asp} or pre-tRNA^{Asp}, and [E·L] indicates the concentration of ligand

in complex with RNase P, measured as the fraction of the total radioactivity ($[L]_{total}$) observed in the eluate.

$$[E\cdot L]/[L]_{total} = 1/(1 + K_D/[E]_{total}) \quad (1)$$

The holoenzyme single-turnover results were analyzed assuming a mechanism of two consecutive irreversible first-order reactions by a three-dimensional fit of the data to eq 2 using the Systat (Intelligent Software) curve-fitting program, where [E] (enzyme concentration) and t (time) are the independent variables and product concentration, [P], is the dependent variable. However, at both high and low enzyme concentrations, the appearance of product approximates a single first-order mechanism. Estimates of k_1[E] (low [E]) and k_2 (high [E]) were also obtained from a fit of these data to eq 3. The values obtained using the two methods were comparable.

$$[P] = [\text{pre-tRNA}]_0\left[1 + \frac{1}{k_1[E] - k_2}(k_2 e^{-k_1[E]t} - k_1[E]e^{-k_2 t})\right] \quad (2)$$

$$[P] = [P]_\infty(1 - e^{-k_{obs}t}) \quad (3)$$

For RNase P RNA, the single-turnover appearance of product was best described by eq 3 in every case. Therefore, the dependence of k_{obs} on [E] was analyzed assuming a rapid equilibrium mechanism, using eq 4, where K_D is the dissociation constant for pre-tRNA^{Asp}.

$$k_{obs} = k_2[E]/(K_D + [E]) \quad (4)$$

RESULTS

Steady-State Kinetics. To assess the functional role of the protein component in RNase P, we first measured the steady-state cleavage of pre-tRNA^{Asp} catalyzed by either RNase P RNA or holoenzyme. Initial rates of pre-tRNA^{Asp} cleavage (≤10% cleaved) were measured under conditions of excess substrate ([S]/[E] ≥ 5) at 37 °C in buffers 1 and 2. The reaction was stopped by a 2-fold dilution into 200 mM EDTA (pH 8) and 10 M urea, and the formation of product was analyzed by denaturing polyacrylamide gel electrophoresis (*16*). The dependence of the initial reaction velocity on the concentration of pre-tRNA^{Asp} (Figure 1A) showed saturation kinetics, so the data were fit to the Michaelis−Menten equation (*23*) yielding values for the steady-state kinetic parameters k_{cat}, K_M, and k_{cat}/K_M (Table 1). The steady-state kinetic parameters for holoenzyme at pH 7.8 are consistent with a previous measurement by Reich and colleagues (*3*). In buffer 1, addition of the protein component increases k_{cat}/K_M by 180-fold and decreases K_M by 120-fold but only slightly affects the value of k_{cat}. Decreasing the pH to 6.1 (buffer 2) has little effect on k_{cat}/K_M for the holoenzyme while the value of k_{cat}/K_M for RNase P RNA decreases more than 10-fold, leading to an even larger (2400-fold) increase in the activity caused by the protein. Smith and Pace (*24*) observed a similar pH dependence of k_{cat}/K_M for RNase P RNA-catalyzed pre-tRNA cleavage measured at high salt concentrations.

Under subsaturating substrate concentrations, the rate constant k_{cat}/K_M sets a lower limit on the second-order rate constant describing substrate association (*23*). For Scheme 1, k_{cat}/K_M includes the rate constants for substrate binding and cleavage, $k_{cat}/K_M = k_1k_2/(k_{-1} + k_2)$. Therefore, the observed increase in k_{cat}/K_M due to addition of the protein component could reflect changes in a number of steps, including a faster association rate constant, higher substrate affinity, or a faster rate constant for the cleavage of E·pre-tRNA^{Asp} to form E·tRNA^{Asp}·5′P. Single-turnover kinetic measurements (see below) are essential to deconvolute the effect of the protein on microscopic rate constants.

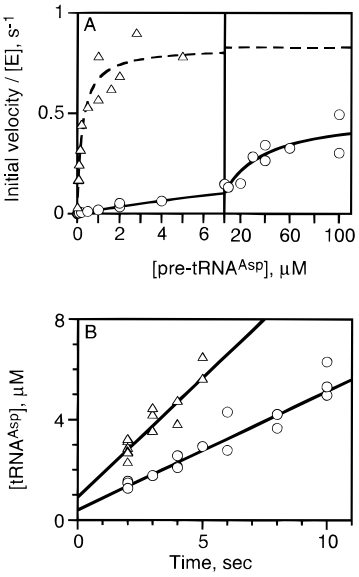

FIGURE 1: Comparison of pre-tRNA^{Asp} cleavage catalyzed by RNase P RNA and holoenzyme under steady-state conditions. (A) RNase P RNA (○) (0.05−0.2 μM or [S]/[E] ≥5 when the substrate concentration was ≤0.2 μM) was incubated with pre-tRNA^{Asp} (0.005−100 μM) in 10 mM $MgCl_2$, 100 mM NH_4Cl, 50 mM Tris-HCl, pH 7.8 (buffer 1), at 37 °C as described (*17*). For holoenzyme-catalyzed reactions (△), RNase P RNA (0.8−10 nM) was preincubated with excess protein (8−30 nM) to form holoenzyme, and then pre-tRNA^{Asp} (0.016−5 μM) was added and incubated under the same conditions. Cleavage of pre-tRNA^{Asp} was assayed on an 8% polyacrylamide gel and quantified using a phosphorimager. The initial velocity (≤10% cleaved) was calculated from a plot of [5′P] versus time. Steady-state kinetic parameters (Table 1) were obtained by fitting the data to the Michaelis−Menten equation (*23*). (B) Time course for the hydrolysis of pre-tRNA^{Asp} (10 μM) catalyzed by 1 μM (○) or 2 μM (△) holoenyzme. Data were fit to the equation for a line, slope/[E] = 0.47 ± 0.01 s^{-1} (1 μM) or 0.48 ± 0.03 s^{-1} (2 μM). The y-intercept provides an estimate of the burst amplitude [0.40 ± 0.05 mol of tRNA/mol of RNase P (1 μM) or 0.45 ± 0.07 mol of tRNA/mol of RNase P (2 μM)].

Under saturating substrate conditions, the observed rate constant k_{cat} sets a lower limit on the first-order rate constants following substrate binding, including cleavage and product dissociation (Scheme 1) (*23*). A time course for cleavage of saturating pre-tRNA^{Asp} catalyzed by RNase P holoenzyme exhibits an initial burst of product formation (Figure 1B). The amplitude of the burst is proportional to holoenzyme concentration with a stoichiometry of 0.45 ± 0.07 mol of tRNA/mol of RNase P as estimated by extrapolation of the data to the *y*-axis; furthermore, the rate constant for turnover (slope/[E] = 0.48 ± 0.03 s^{-1}) is similar to the measured value of k_{cat} (Table 1). This behavior is consistent with any mechanism in which a step after cleavage is at least partially rate-limiting for turnover (*16*, *23*). Single-turnover kinetic measurements under these conditions demonstrate that cleav-

Table 1: List of Kinetic and Thermodynamic Values[a]

	RNase P RNA		holoenzyme	
kinetic parameters	pH 6.1	pH 7.8	pH 6.1	pH 7.8
k_{cat} (s^{-1})[b]	0.03 ± 0.01[c]	0.50 ± 0.06	0.27 ± 0.02	0.83 ± 0.05
k_{cat}/K_M (mM^{-1} s^{-1})[b]	1.4 ± 0.1	19 ± 4	3400 ± 600	3500 ± 700
K_M (μM)[b]	21 ± 9[c]	27 ± 8	0.08 ± 0.02	0.23 ± 0.06
burst amplitude[b]	–	–	<0.1	0.45 ± 0.07
$K_D^{pre-tRNA}(Mg^{2+})$ (μM)	60 ± 20[d]	–	0.006 ± 0.005[e]	–
$K_D^{pre-tRNA}(Ca^{2+})$ (μM)[f]	4 ± 1	–	0.0004 ± 0.0002	–
$K_D^{tRNA}(Mg^{2+})$ (μM)[f]	12 ± 3	3.2 ± 0.5	1.2 ± 0.1	0.47 ± 0.08
$K_D^{tRNA}(Ca^{2+})$ (μM)[f]	0.3 ± 0.1	0.11 ± 0.02	0.20 ± 0.06	0.06 ± 0.02

[a] Measured at 10 mM $MgCl_2$ or $CaCl_2$, 100 mM NH_4Cl and 37 °C. [b] Measured as described in the legend of Figure 1. [c] Steady-state kinetic parameters k_{cat} and K_M for the RNase P RNA-catalyzed reaction at pH 6.1 are extrapolated from kinetic measurements up to 10 μM pre-tRNA^{Asp}. [d] Determined from transient kinetic measurements, as described in the legend of Figure 4. [e] Calculated from the ratio k_{-1}/k_1 as described in the legends of Figures 2 and 3. [f] Measured as described in the legend of Figure 5.

Scheme 1[a]

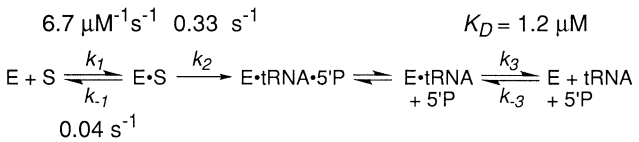

[a] E = RNase P holoenzyme; S = pre-tRNA^{Asp} (10 mM $MgCl_2$, 100 mM NH_4Cl, pH 6.1, 37 °C).

age is nearly 10-fold faster than turnover ($k_2^{pH\ 8}$ = 6.3 ± 0.6 s^{-1}; Kurz and Fierke, unpublished results), suggesting that k_3 (product dissociation) is the main rate-limiting step. The calculated burst amplitude [burst amplitude ≈ $(k_2/(k_2 + k_3))^2$] (*23*) for these rate constants is 0.8 mol of tRNA/mol of RNase P, which is larger than the experimentally determined amplitude of 0.45 mol of tRNA/mol of RNase P. This discrepancy is likely due to a number of experimental factors, including error in determining the concentration of active enzyme and in extrapolating to zero time. For the reaction of RNase P RNA in buffer 1, the steady-state kinetics were not measured at sufficiently high concentrations of enzyme to detect a burst. However, the rate constant for product dissociation cannot be less than k_{cat} (0.5 s^{-1}, Table 1), suggesting that addition of the protein component increases k_3 by <2-fold in buffer 1.

When the pH is reduced to 6.1 (buffer 2), pre-tRNA^{Asp} cleavage becomes the main rate-contributing step as indicated by the following: (1) the absence of a pre-steady-state burst (<0.1 mol of tRNA^{Asp}/mol of RNase P) in a time course of pre-tRNA^{Asp} cleavage catalyzed by RNase P holoenzyme (10 μM pre-tRNA^{Asp}, 2 μM holoenzyme; data not shown); and (2) a k_{cat} that is similar to k_2, as determined by single-turnover methods (see below). For the RNase P RNA-catalyzed reaction at pH 6.1, k_{cat} (0.03 ± 0.01 s^{-1}) was estimated by extrapolation from low pre-tRNA^{Asp} concentrations ([pre-tRNA^{Asp}] ≤10 μM). In this case, k_{cat} is also similar to k_2 determined by single-turnover methods. Therefore, addition of the protein component appears to increase the cleavage rate constant in buffer 2 almost 10-fold, as approximated by k_{cat}.

RNase P Holoenzyme Single-Turnover Kinetics. To isolate the pre-tRNA^{Asp} association and hydrolysis steps, single-turnover kinetics ([E]/[S] ≥ 5) of the holoenzyme-catalyzed reaction were measured at pH 6.1 where cleavage is slow enough that the data can be collected using manual mixing. The single-turnover kinetics of RNase P holoenzyme measured at low salt are very similar to the kinetics of the RNase P RNA-catalyzed reaction at high salt (*16*). At low concentrations of holoenzyme ([E] < 10 nM), pre-tRNA^{Asp} cleavage occurs as a single-exponential decay (Figure 2A), and the observed rate constant is linearly dependent on the concentration of enzyme. At intermediate concentrations of holoenzyme (10−200 nM), the data are not well described by a single-exponential decay due to a lag in product formation at short times (Figure 2B). Observation of a lag under these conditions is consistent with any mechanism including two irreversible first-order or pseudo-first-order steps (Scheme 1, $k_2 > k_{-1}$) (*21*). The initial lag at short

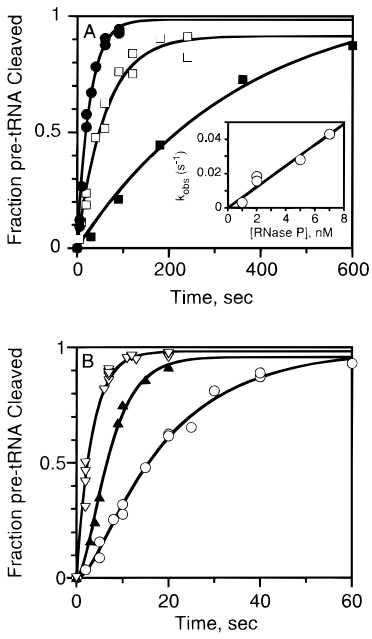

FIGURE 2: Single-turnover measurements of RNase P holoenzyme-catalyzed cleavage of pre-tRNA^{Asp}. End-labeled pre-tRNA^{Asp} (0.3−8 nM) was mixed with excess holoenzyme (0.001−5 μM RNA, 0.021−5.02 μM protein) and incubated in buffer 2. (A) At low concentrations of RNase P (<10 nM), data were fit to a single-exponential decay (eq 3) [1 nM (■), 2 nM (□), and 7 nM (●) RNase P holoenzyme]. An estimate of the association rate constant k_1 (6.1 ± 0.3 μM^{-1} s^{-1}) was obtained from the slope of a plot of the observed rate constants (k_{obs}) versus [E] (inset). (B) At intermediate concentrations of RNase P (10−200 nM), the data were best described by a mechanism of two consecutive irreversible first-order processes [10 nM (○) and 40 nM (▲) RNase P holoenzyme]. Values for k_1 and k_2 (Scheme 1) were obtained from a three-dimensional fit of all of the data to a double-exponential (eq 2). Alternatively, k_2 [0.30 ± 0.01 s^{-1}; 1 μM (▽) RNase P holoenzyme] was estimated by fitting the data at high [E] (≥400 nM) to eq 3.

Scheme 2

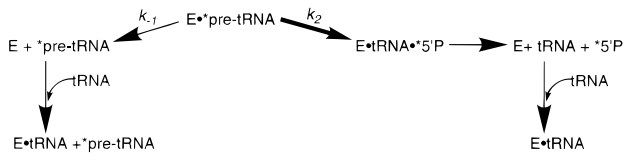

times is characterized by the rate constant k_1[E] due to buildup of the E•pre-tRNA^{Asp} binary complex. This is followed by an exponential decay of the binary complex to products with a rate constant equal to k_2. At high holoenzyme concentrations (≥400 nM), the lag in product formation nearly disappears (Figure 2B). Under these conditions, the cleavage rate constant is independent of [E], indicating that a first-order step after pre-tRNA^{Asp} binding is rate-limiting, such as pre-tRNA^{Asp} cleavage. A value for k_1 (6.1 ± 0.3 μM^{-1} s^{-1}) was determined directly from the plot of k_{obs} versus low concentrations of holoenzyme (Figure 2A, inset) while k_{obs} at high concentrations of holoenzyme provides an estimate of k_2 (0.30 ± 0.01 s^{-1}; 1 μM holoenzyme). Similar values for k_1 and k_2 (6.7 ± 0.2 μM^{-1} s^{-1} and 0.33 ± 0.01 s^{-1}, respectively) were also calculated by a three-dimensional fit of the single-turnover data at all of the enzyme concentrations to a mechanism of two consecutive irreversible first-order processes using a double exponential equation (eq 2) (*21*). The rate constant for pre-tRNA^{Asp} binding to RNase P holoenzyme under these conditions is similar to both (1) the association rate constant for binding pre-tRNA^{Asp} to RNase P RNA at high salt (*16*) and (2) the values for k_{cat}/K_M for holoenzyme (Table 1), consistent with the assumption that substrate binding is essentially irreversible ($k_2 > k_{-1}$). The measured cleavage rate constant k_2 for the holoenzyme-catalyzed reaction at pH 6.1 (Scheme 1) is about 18-fold slower than that determined for RNase P RNA-catalyzed hydrolysis at pH 7.8 and high salt (100 mM $MgCl_2$, 800 mM NH_4Cl) and about 5-fold slower than at pH 7.8 and 10 mM Mg^{2+} (1.07 M NH_4Cl) (*17*) likely due to the pH dependence of the cleavage step (*24*).

To further test this kinetic model, we estimated the rate constant for dissociation of pre-tRNA^{Asp} from RNase P holoenzyme (k_{-1}) from the partitioning of the E•pre-tRNA^{Asp} complex between products and reactants (Scheme 2) (*16, 25*). This was accomplished by mixing labeled pre-tRNA^{Asp} with a high concentration of holoenzyme (400 nM) to rapidly form E•*pre-tRNA^{Asp}. The reaction was then diluted 10-fold into an enzyme "trapping" solution consisting of 100 μM tRNA that quickly binds to free holoenzyme and thus inhibits the reaction with free *pre-tRNA^{Asp} but does not disrupt the reaction of the E•*pre-tRNA^{Asp} complex. This mixture was incubated at 37 °C for several half-lives (14 s) to allow the E•*pre-tRNA^{Asp} complex to partition between dissociation and cleavage before the reaction was completely stopped by the addition of EDTA/urea. After incubating pre-tRNA^{Asp} with holoenzyme for 2 s, 87% of the pre-tRNA^{Asp} is cleaved when the reaction is incubated with the tRNA trap followed by addition of EDTA/urea; however, only 30−40% of the substrate is cleaved when the reaction is stopped by the addition of EDTA/urea at 2 s (Figure 3). This increase in product formation observed with the tRNA trap demonstrates that cleavage of the E•*pre-tRNA^{Asp} complex is more rapid than substrate dissociation. An estimate of the rate constant for dissociation of pre-tRNA^{Asp} from RNase P

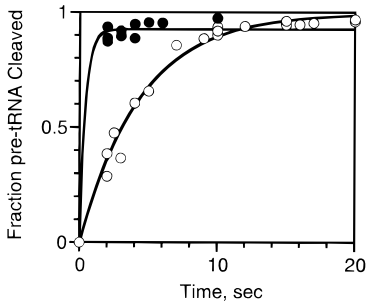

FIGURE 3: Partitioning of the E•pre-tRNA^{Asp} complex as assayed by tRNA trap experiment (*16*). End-labeled pre-tRNA^{Asp} (1−2 nM) was added to holoenzyme (400 nM RNA, 420 nM protein), and after incubation for 2−10 s (t_1), the reaction was either mixed with 1 volume of 0.2 M EDTA (pH 8)/10 M urea (○) to stop the reaction or diluted (1:10) into 100 μM unlabeled tRNA (●) for 14 s (t_2) followed by addition of EDTA/urea. Addition of excess tRNA traps free E as E•tRNA to inhibit further reaction with free *pre-tRNA^{Asp}, while allowing the E•*pre-tRNA^{Asp} complex to react during t_2. Both sets of data were fit to a single exponential (eq 3).

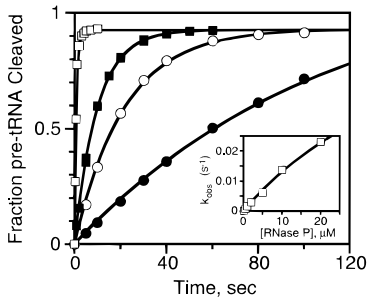

FIGURE 4: Single-turnover measurements of RNase P RNA-catalyzed cleavage of pre-tRNA^{Asp}. End-labeled pre-tRNA^{Asp} (2 nM) was mixed with excess RNase P RNA (0.1−20 μM) and incubated in buffer 2 (pH 6.1). For each concentration of RNase P RNA, the data were fit to a single-exponential decay (eq 3) [0.1 μM (●), 0.5 μM (○), 1 μM (■), and 20 μM (□) RNase P RNA]. The observed rate constant was plotted against [E] (inset), and these data were fit to eq 4 to obtain estimates of the K_D for pre-tRNA^{Asp} and k_2 (Table 1).

holoenzyme (k_{-1}) of 0.04 ± 0.03 s^{-1} was obtained from the ratio of the cleaved products in the tRNA trap compared to the EDTA/urea data using eq 5 (*16, 25*):

$$[P]_{obs}/[P]_\infty = 0.89 \pm 0.02 = k_2/(k_2 + k_{-1}) \qquad (5)$$

where $[P]_{obs}$ is the fraction of pre-tRNA^{Asp} cleaved at 1 s when [E•*pre-tRNA^{Asp}] is maximal (approximated by extrapolation of the tRNA quench data to 1 s; $[P]_{obs}$ = 85.4%); $[P]_\infty$ is the end point in the EDTA/urea quench (95.8%); and k_2 is 0.33 s^{-1} (Scheme 1). Simulations of the tRNA trap data using the Kinsim simulation program (*26−28*) and the measured values of k_1 and k_2 (Scheme 1) further constrain the value of k_{-1} to ≤0.05 s^{-1}. From these results, the value of the dissociation constant for binding of pre-tRNA^{Asp} can be estimated from the ratio k_{-1}/k_1 = 6 ± 5 nM, assuming a simple bimolecular reaction.

RNase P RNA Single-Turnover Kinetics. To identify the role of the protein component in pre-tRNA^{Asp} binding and cleavage, we measured the single-turnover kinetics of RNase P RNA under the same buffer conditions used to investigate the holoenzyme kinetics (Figure 4). Under these conditions, the single-turnover kinetics of RNase P RNA-catalyzed pre-tRNA^{Asp} cleavage are best described by a rapid equilibrium mechanism ($k_{-1} > k_2$) in which equilibration of RNase P

RNA and pre-tRNA^{Asp} occurs on a fast time scale followed by rate-limiting decay of the binary complex to products. This conclusion is based on two lines of evidence: (1) the absence of a lag in product formation at any concentration of RNase P RNA (measured up to 20 μM RNase P RNA); and (2) the pH dependence of the steady-state parameter k_{cat}/K_M. As illustrated by the kinetics of the holoenzyme, so long as $k_2 > k_{-1}$, k_{cat}/K_M reflects the rate constant for substrate association. However, when $k_2 < k_{-1}$, the value of k_{cat}/K_M is sensitive to changes in all of the rate constants for cleavage and binding of substrate. Single-turnover kinetic measurements of the RNase P RNA-catalyzed reaction at high salt demonstrate no significant pH dependence of the association rate constant k_1 [$k_1^{pH\ 8} = 3.3\ \mu M^{-1}\ s^{-1}$ (*16*), $k_1^{pH\ 6} = 2.7\ \mu M^{-1}\ s^{-1}$; Crary and Fierke, unpublished results] while k_2 varies with pH (*24*). The decrease in k_{cat}/K_M at lower pH, therefore, is most consistent with $k_2 < k_{-1}$. Using the rapid equilibrium assumption, the dependence of the single-turnover k_{obs} on RNase P RNA concentration (Figure 4, inset) was fit to eq 4 in which $K_{1/2}$ (60 $\pm$ 20 μM) approximates the dissociation constant for pre-tRNA^{Asp} binding to RNase P RNA. Furthermore, extrapolation of this curve to high concentrations of RNase P RNA provides an estimate for the value of the cleavage rate constant (k_2) of 0.09 $\pm$ 0.04 s^{-1}. These results indicate that the protein component increases substrate binding affinity by as much as 10^4-fold but has only a modest effect on the cleavage rate constant ($\leq$10-fold).

Dissociation Constant of Pre-tRNA^{Asp} in Ca^{2+}. To confirm the effect of the protein on substrate affinity, we directly measured a binding isotherm for pre-tRNA^{Asp}, substituting 10 mM $CaCl_2$ for $MgCl_2$ to decrease the rate constant of the cleavage reaction. Both tRNA (*29*, *30*) and protein (*31*) bind to RNase P RNA as effectively in Ca^{2+} as in Mg^{2+}. Furthermore, identical intramolecular cross-linking patterns are obtained for *E. coli* RNase P RNA in the presence of Mg^{2+} and Ca^{2+} (*32*). These results indicate that Ca^{2+} promotes proper RNA folding. However, the cleavage rate constant for the RNase P RNA-catalyzed processing reaction is reduced by $\sim 10^4$-fold when Ca^{2+} replaces Mg^{2+} (*24*).

To determine whether Ca^{2+} similarly decreases the cleavage rate constant of the holoenzyme, we measured the observed rate constant for pre-tRNA^{Asp} cleavage under single-turnover conditions as 1.8 ($\pm$0.3) $\times$ 10^{-5} s^{-1} for 20 nM holoenzyme in 10 mM $CaCl_2$, 100 mM NH_4Cl, pH 6.1 (data not shown). This observed rate constant is unchanged when the concentration of holoenzyme is increased to 400 nM, indicating that a first-order step, likely cleavage, is rate-limiting. This rate constant is decreased 10^4-fold compared to k_2 in 10 mM $MgCl_2$ (Scheme 1), similar to the decrease observed for RNase P RNA at high salt (*24*). Furthermore, the observed rate constant for cleavage of pre-tRNA^{Asp} catalyzed by 10 μM RNase P RNA is 6-fold smaller [3.1 ($\pm$0.3) $\times$ 10^{-6} s^{-1}], demonstrating that the protein component forms a functional complex with RNase P RNA in Ca^{2+}.

The affinity of RNase P RNA and holoenzyme for pre-tRNA^{Asp} in 10 mM $CaCl_2$, 100 mM NH_4Cl (pH 6.1) was measured using G-75 Sephadex gel-filtration centrifuge columns to separate free pre-tRNA^{Asp} from E·pre-tRNA^{Asp} (*16*). In this buffer, $\leq$2% of the pre-tRNA^{Asp} is cleaved by 400 nM holoenzyme during the equilibration period of 10 min. The fraction of labeled pre-tRNA^{Asp} bound as a function of enzyme concentration (Figure 5A) was quantified and used to determine $K_D^{pre-tRNA}$ (Table 1). These data indicate that the protein component increases the affinity of RNase P for pre-tRNA^{Asp} in $CaCl_2$ by a factor of 10^4-fold, from 4 $\pm$ 1 μM for RNase P RNA to 0.4 $\pm$ 0.2 nM for holoenzyme. This is comparable to the increased affinity of the holoenzyme for pre-tRNA^{Asp} in 10 mM $MgCl_2$ (Table 1). However, the affinities of both RNase P RNA and holoenzyme for pre-tRNA^{Asp} increase about 10-fold in 10 mM $CaCl_2$ compared to 10 mM $MgCl_2$ (Table 1).

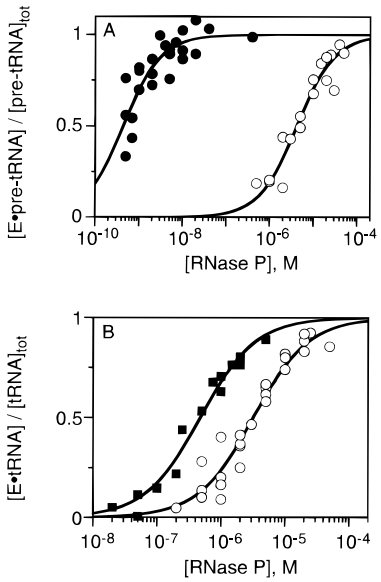

FIGURE 5: Measurement of the dissociation constants for binding of precursor and mature tRNA^{Asp} to RNase P RNA or holoenzyme. (A) End-labeled pre-tRNA^{Asp} (0.1−0.2 nM) was mixed with excess holoenzyme (●) (0.5−400 nM RNA, 20.5−420 nM protein) or RNase P RNA (○) (1−40 μM) and incubated at 37 °C for 10 min in buffer 2 containing 10 mM $CaCl_2$ in place of $MgCl_2$. The E·pre-tRNA^{Asp} complex was separated from free pre-tRNA^{Asp} by gel filtration over a G-75 Sephadex centrifuge column (*16*). Dissociation constants (Table 1) were calculated by fitting these data to eq 1. (B) Uniformly labeled tRNA^{Asp} (0.1 nM) was mixed with excess holoenzyme (■) (0.02−6 μM RNA, 0.04−6.02 μM protein) or RNase P RNA (○) (0.25−20 μM) and incubated in buffer 1 at 37 °C for 10−60 min prior to centrifugation. The results were analyzed as described for binding studies with pre-tRNA^{Asp}.

Dissociation Constant for tRNA^{Asp}. To test whether the protein component has a generalized effect on ligand binding to RNase P, we compared the thermodynamic affinities of RNase P for product tRNA^{Asp} in the presence and absence of the protein component. To measure the dissociation constant, K_D^{tRNA}, uniformly labeled tRNA^{Asp} was incubated with excess RNase P RNA or holoenzyme in buffer 1, and the centrifuge column assay was used to separate E·tRNA^{Asp} from free tRNA^{Asp}. Addition of the protein component moderately stabilizes the interaction between RNase P and tRNA^{Asp}, decreasing K_D^{tRNA} by 7-fold at pH 7.8 (Figure 5B, Table 1) and 10-fold at pH 6.1 (Table 1). However, this decrease is much smaller than the 10^4-fold effect observed for pre-tRNA^{Asp}. These results are consistent with our steady-state kinetic data, demonstrating that the protein has no significant effect on product dissociation. The tRNA^{Asp} dissociation constants are not particularly sensitive to pH (Table 1); however, Ca^{2+} appears to have an overall stabilizing effect on ligand binding to RNase P, decreasing

K_D^{tRNA} by 6−8-fold for holoenzyme and up to 40-fold for RNase P RNA (Table 1).

DISCUSSION

Function of Protein Component. A combined kinetic and thermodynamic approach was used to define a functional role for the protein component of *B. subtilis* RNase P in catalysis of pre-tRNA^{Asp} cleavage. Our results demonstrate that addition of the protein component enhances the binding of pre-tRNA^{Asp} to RNase P by 5.6 kcal/mol at 37 °C while only modestly increasing the stability of the E·tRNA^{Asp} complex (1.4 kcal/mol) and decreasing the free-energy barrier for E·pre-tRNA^{Asp} conversion to E·tRNA^{Asp}·5′P ($\leq$1.5 kcal/mol) (10 mM $MgCl_2$, 100 mM NH_4Cl, pH 6.1). These findings are consistent with previous kinetic data comparing the holoenzyme and RNA-catalyzed reactions, although previous studies underestimated the differential effect of the protein on pre-tRNA and mature tRNA binding. Tallsjö and Kirsebom (*33*) observed that the protein component does not affect the cleavage rate constant for processing of pre-tRNA^{Tyr}Su3 by *E. coli* RNase P, but does increase substrate binding affinity, as reflected in a 50-fold decrease in $K_{1/2}$ for the dependence of the single-turnover k_{obs} on enzyme concentration; in this case, the decrease in $K_{1/2}$ likely underestimates the effect on substrate binding because $K_{1/2}$ does not necessarily equal K_D (*23*). In addition, Tallsjö and Kirsebom (*33*) and Reich and colleagues (*3*) observed that inhibition by mature tRNA was significantly less severe for the cleavage reaction catalyzed by RNase P holoenzyme at low salt compared to the reaction catalyzed by RNase P RNA at high salt. This observation is consistent with our conclusion that the protein does not significantly increase product affinity. The protein component thus allows the pre-tRNA substrate to bind tightly for efficient catalysis at low Mg^{2+} concentration while minimizing product inhibition.

This discrimination between tRNA and pre-tRNA cannot be fully explained by generalized effects of the protein on RNA structure. Compared to the group I intron, the bacterial RNase P RNA folding pathway is similarly complex, involving multiple folding intermediates (*11, 34*−*37*) and independently folding subdomains (*38*−*40*). Moreover, the protein dependence of both yeast mitochondrial bI5 intron self-splicing (*41*) and RNase P RNA-catalyzed pre-tRNA cleavage (*2*) is partially suppressed in vitro by high concentrations of Mg^{2+}. In the case of the bI5 group I intron, this effect is due to Mg^{2+}-induced folding of the intron catalytic core (*42*). However, *E. coli* and *B. subtilis* RNase P RNAs are essentially fully folded at equilibrium in 6 mM Mg^{2+} (*38, 40*), and the stimulatory effect is mainly due to the Mg^{2+} dependence of the interaction between RNase P RNA and pre-tRNA (*17*). Thus, Westhof and colleagues (*15*) proposed that the protein component could have subtle effects on RNase P RNA folding, constraining the RNA to a more "compact" tertiary structure. Conceivably, the protein could promote more efficient interactions of the RNA with its ligands by binding to a site far removed from the active site. Along these lines, we previously suggested that protein binding could stabilize specific Mg^{2+} sites essential for the interactions with substrate and products, thereby increasing the affinity of RNase P for these ligands (*17*). However, we propose that our current results do not indicate that the primary role of the protein is to stabilize the overall structure of the RNA component since this should be expressed mainly in a general, rather than differential, increase in ligand binding affinity.

Our results are most consistent with a model in which the protein binds to RNase P RNA and enhances interactions between RNase P and the 5′-precursor segment of pre-tRNA. This interaction could either be due to direct contacts between the 5′-leader sequence and the protein or be due to a protein-induced conformational change leading to favorable contacts between the 5′-precursor segment and RNase P RNA. Tertiary structural probing of RNase P RNA by enzymatic footprinting (*14*), dimethyl sulfate protection (*13*), or reactivity with Fe(II)EDTA-generated hydroxyl radicals (*15*) indicates that the overall tertiary conformation of the RNA is essentially unchanged by the addition of the protein, while particular structural elements become more or less accessible to solvent. Therefore, the protein may cause limited conformational changes in specific regions of the RNA, perhaps consistent with an indirect effect of the protein. However, preliminary data indicate that the 5′-precursor of pre-tRNA can form photo-cross-links with azidophenacyl-labeled RNase P protein (Niranjanakumari and Fierke, unpublished results), suggesting a direct contact. Alignment of known RNase P protein sequences reveals eight conserved basic residues (*43*) that could participate in direct interactions with the 5′ end of pre-tRNA through electrostatic contacts or hydrogen-bonding with the ribose−phosphate backbone. All of these data taken together suggest that a direct contact between the protein and pre-tRNA is plausible; however, more detailed biochemical and structural studies will be required to fully elucidate the mechanism of the enhancement of pre-tRNA affinity by the protein component.

In Vivo Consequences. Studies of bacterial tRNA biosynthesis clearly demonstrate that tRNA precursors in the cell occur transiently (*44, 45*), suggesting that the steady-state concentration of these precursors is very low. In contrast, excess concentrations of mature tRNA are maintained in the bacterial cell as part of its normal metabolism (*46*). Our results indicate that RNase P is perfectly suited to operate in this metabolic niche. Under conditions of subsaturating substrate, the specific stabilization of the E·pre-tRNA^{Asp} complex by the enzyme ensures that essentially every substrate molecule that binds to RNase P will be converted to products, since cleavage is faster than dissociation of substrate. On the other hand, by maintaining a weak interaction with the tRNA product, the enzyme avoids decreased catalysis due to (1) a lowered k_{cat} caused by slow product dissociation and (2) significant product inhibition. High product affinity results in a lowered k_{cat} value for both the steady-state cleavage of pre-tRNA catalyzed by RNase P RNA at high salt concentrations (*3, 16, 33*) and the cleavage of oligonucleotide substrates by L-21 *Sca*I RNA, a multiple-turnover ribozyme engineered from the *Tetrahymena* group I intron (*47*). In the case of the group I intron, product inhibition is irrelevant to the consideration of its efficiency in vivo because the intron catalyzes only a single turnover. However, because RNase P catalyzes multiple turnovers in vivo, the ability of the holoenzyme to discriminate between pre-tRNA and tRNA may be critical to avoid inhibition of its processing activity due to high concentrations of tRNA.

Comparisons with Protein Catalysts. In a recent review, Narlikar and Herschlag (*48*) convincingly argue that mechanistic studies of ribozymes can provide fresh insights into the fundamental principles of biological catalysis. The most efficient ribozymes, such as RNase P RNA and group I introns, achieve rate enhancements for phosphodiester bond cleavage that are comparable to many protein enzymes ($\approx 10^{11}$-fold) by tightly binding and precisely positioning their substrates for catalysis (*48*). On the other hand, these ribozymes suffer as catalysts in multiple-turnover reactions due to the complications of slow product dissociation and product inhibition. Furthermore, many protein enzymes achieve rate enhancements of up to 10^{17}-fold, far surpassing the catalytic proficiency of ribozymes (*49*). To explain these observations, Narlikar and Herschlag (*48*) contend that "rigidity" is indispensable in an enzyme, proposing that the limitations of RNA packing lead to a fundamental weakness in RNA catalysis. Because of their greater conformational rigidity and side chain diversity, proteins excel at modulating the relative specificity of their interactions with substrates, products, and transition states, while RNA may be less adept at making these subtle distinctions. Our results are consistent with this proposal, as we have shown that RNase P is a much more sophisticated catalyst in the presence of its protein than in its absence, able to catalyze pre-tRNA cleavage at the diffusion-controlled limit under physiological conditions and to selectively bind substrate, but not product, with high affinity.

Pace and Brown (*1*) have suggested that the ancestral RNase P activity may have consisted entirely of RNA. Thus, the protein component may have been subsequently acquired in response to selective pressures for maximizing catalytic efficiency, especially at physiological conditions. Our data suggest that the current ribonucleoprotein composition of bacterial RNase P may reflect the attainment of catalytic "perfection" (*50*) since the cleavage reaction is limited mainly by the association rate constant at subsaturating concentrations of pre-tRNA^{Asp}. This achievement of high catalytic efficiency by RNase P may provide a partial explanation for the retention of the catalytic RNA in this enzyme. In any case, our results further supplement the observed mechanistic parallels between RNase P and protein enzymes, and reinforce the idea that mechanistic studies of ribozymes will yield insights into the fundamental principles of biological catalysis.

ACKNOWLEDGMENT

We thank Sharon M. Crary for providing helpful advice. We also thank Dr. Norman Pace for giving us useful plasmids.

REFERENCES

1. Pace, N. R., and Brown, J. W. (1995) *J. Bacteriol. 177*, 1919.
2. Guerrier-Takada, C., Gardiner, K., Marsh, T., Pace, N., and Altman, S. (1983) *Cell 35*, 849.
3. Reich, C., Olsen, G. J., Pace, B., and Pace, N. R. (1988) *Science 239*, 178.
4. Kole, R., Baer, M. F., Stark, B. C., and Altman, S. (1980) *Cell 19*, 881.
5. Cech, T. R. (1990) *Annu. Rev. Biochem. 59*, 543.
6. Lambowitz, A. M., and Perlman, P. S. (1990) *Trends Biochem. Sci. 15*, 440.
7. Saldanha, R., Mohr, G., Belfort, M., and Lambowitz, A. M. (1993) *FASEB J. 7*, 15.
8. Caprara, M. G., Mohr, G., and Lambowitz, A. M. (1996) *J. Mol. Biol. 257*, 512.
9. Mohr, G., Caprara, M. G., Guo, Q., and Lambowitz, A. M. (1994) *Nature 370*, 147.
10. Shaw, L. C., and Lewin, A. S. (1995) *J. Biol. Chem. 270*, 21552.
11. Weeks, K. M., and Cech, T. R. (1996) *Science 271*, 345.
12. Kim, J. J., Kilani, A. F., Zhan, X., Altman, S., and Liu, F. (1997) *RNA 3*, 613.
13. Talbot, S. J., and Altman, S. (1994) *Biochemistry 33*, 1399.
14. Vioque, A., Arnez, J., and Altman, S. (1988) *J. Mol. Biol. 202*, 835.
15. Westhof, E., Wesolowski, D., and Altman, S. (1996) *J. Mol. Biol. 258*, 600.
16. Beebe, J. A., and Fierke, C. A. (1994) *Biochemistry 33*, 10294.
17. Beebe, J. A., Kurz, J. C., and Fierke, C. A. (1996) *Biochemistry 35*, 10493.
18. Sambrook, J., Fritsch, E. F., and Maniatis, T. (1989) in *Molecular Cloning: A Laboratory Manual*, 2nd ed., pp 6.36 and 18.47, Cold Spring Harbor Laboratory Press, Plainview, NY.
19. Laemmli, U. K. (1970) *Nature 227*, 680.
20. Penefsky, H. S. (1979) *Methods Enzymol. 56*, 527.
21. Fierke, C. A., and Hammes, G. G. (1995) *Methods Enzymol. 249*, 3.
22. Johnson, K. A. (1992) *Enzymes (3rd Ed.) 20*, 1.
23. Fersht, A. (1985) in *Enzyme Structure and Mechanism*, p 99, W. H. Freeman, New York.
24. Smith, D., and Pace, N. R. (1993) *Biochem. 32*, 5273.
25. Rose, I. A. (1980) *Methods Enzymol. 64*, 47.
26. Barshop, B. A. (1983) *Anal. Biochemistry 130*, 134.
27. Frieden, C. (1993) *Trends Biochem. Sci. 18*, 58.
28. Frieden, C. (1994) *Trends Biochem. Sci. 19*, 181.
29. Hardt, W.-D., Schlegl, J., Erdmann, V. A., and Hartmann, R. K. (1993) *Nucleic Acids Res. 21*, 3521.
30. Smith, D., Burgin, A. B., Haas, E. S., and Pace, N. R. (1992) *J. Biol. Chem. 267*, 2429.
31. Talbot, S. J., and Altman, S. (1994) *Biochemistry 33*, 1406.
32. Harris, M. E., Kazantsev, A. V., Chen, J.-L., and Pace, N. R. (1997) *RNA 3*, 561.
33. Tallsjö, A., and Kirsebom, L. A. (1993) *Nucleic Acids Res. 21*, 51.
34. Pan, T., and Sosnick, T. R. (1997) *Nat. Struct. Biol. 4*, 931.
35. Zarrinkar, P., Wang, J., and Williamson, J. R. (1996) *RNA 2*, 564.
36. Zarrinkar, P. P., and Williamson, J. R. (1996) *Nat. Struct. Biol. 3*, 432.
37. Zarrinkar, P. P., and Williamson, J. R. (1994) *Science 265*, 918.
38. Loria, A., and Pan, T. (1996) *RNA 2*, 551.
39. Murphy, F. L., and Cech, T. R. (1993) *Biochemistry 32*, 5291.
40. Pan, T. (1995) *Biochemistry 34*, 902.
41. Weeks, K. M., and Cech, T. R. (1995) *Biochemistry 34*, 7728.
42. Weeks, K. M., and Cech, T. R. (1995) *Cell 82*, 221.
43. Kirsebom, L. A., and Vioque, A. (1996) *Mol. Biol. Rep. 22*, 99.
44. Li, Z., and Deutscher, M. P. (1996) *Cell 86*, 503.
45. Pace, B., Peterson, R. L., and Pace, N. R. (1970) *Proc. Natl. Acad. Sci. U.S.A. 65*, 1097.
46. Söll, D. (1993) in *The RNA World* (Gesteland, R. F., and Atkins, J. F., Ed.) p 157, Cold Spring Harbor Laboratory Press, Plainview, NY.
47. Herschlag, D., and Cech, T. R. (1990) *Biochemistry 29*, 10159.
48. Narlikar, G. J., and Herschlag, D. (1997) *Annu. Rev. Biochem. 66*, 19.
49. Radzicka, A., and Wolfenden, R. (1995) *Science 267*, 90.
50. Albery, W. J., and Knowles, J. R. (1976) *Biochemistry 15*, 5631.

BI972530M